An Efficient Algorithm for Fast Parasitic Extraction and Passive Order Reduction of 3D Interconnect Models

Nuno Marques[+] Mattan Kamon[*] Jacob White[*] L. Miguel Silveira[+]

nacm@algos.inesc.pt {matt,white}@rle-vlsi.mit.edu lms@inesc.pt

[+] INESC/Cadence European Laboratories
Dept. of Electrical and Computer Engineering
Instituto Superior Técnico
1000 Lisboa, Portugal

[*] Research Laboratory of Electronics
Dept. of Electrical Eng. and Comp. Science
Massachusetts Institute of Technology
Cambridge, MA 02139

Abstract

As VLSI circuit speeds have increased, the need for accurate three-dimensional interconnect models has become essential to accurate chip and system design. In this paper, we describe an integral equation approach to modeling the impedance of interconnect structures accounting for both the charge accumulation on the surface of conductors and the current traveling along conductors. Unlike previous methods, our approach is based on a modified nodal analysis formulation and can be used directly to generate guaranteed passive low order interconnect models for efficient inclusion in a standard circuit simulator.

1 Introduction

As VLSI circuit speeds have increased, the need for accurate interconnect models has become essential to accurate chip and system design. Recently, much work has been directed at rapidly solving for the inductance or capacitance of these structures, starting directly from Maxwell's equations [1, 2]. However inductance and capacitance are not necessarily decoupled quantities, and for higher frequencies a distributed model is necessary. In this paper, we describe an integral equation approach to modeling the impedance of interconnect structures accounting for both the charge accumulation on the surface of conductors and the current traveling along conductors. While such computations by themselves are not new, we show that with our approach, based on a modified nodal analysis formulation, it is possible to generate guaranteed passive low order models for efficient inclusion in a circuit simulator such as SPICE. Additionally, the algorithm is ripe for acceleration techniques such as the Fast Multipole Method [1, 3] or the Precorrected-FFT [4] approach allowing the analysis of larger, more complex three-dimensional geometries. In Section 2 we discuss the integral formulation and discretization from which we derive the large dense linear system describing the interconnect. In Section 3 we describe applying recent model order reduction techniques to our formulation in order to directly generate passive reduced-order models. In Section 4, we present results of using the new formulation, and in Section 5 we present some conclusions.

2 Formulation

Parasitic extraction for a set of conductors involves determining the relation between the terminal (or port) currents and the terminal voltages. For a k terminal-pair problem in the sinusoidal steady-state at the frequency ω, this relation is described by the admittance matrix, $\boldsymbol{Y}_t(\omega) \in \mathbb{C}^{k\times k}$,

$$\boldsymbol{Y}_t(\omega)\boldsymbol{V}_t(\omega) = \boldsymbol{I}_t(\omega), \tag{1}$$

where $\boldsymbol{I}_t, \boldsymbol{V}_t \in \mathbb{C}^k$ are vectors of the terminal current and voltage phasors, respectively [5]. Note that column i of $\boldsymbol{Y}_t$ can be computed by setting entry i of $\boldsymbol{V}_t$ to one, the rest to zero, and then computing the resulting current vector $\boldsymbol{I}_t$. The i^{th} column of $\boldsymbol{Y}_t$ is then given by $\boldsymbol{I}_t$.

In order to do that, we need to compute the resulting currents given a set of potentials. To that end, we turn to an integral equation approach derived directly from Maxwell's equations and a discretization operation similar to the Partial Element Equivalent Circuit (PEEC) approach [6]. However, after generating the large linear circuit describing the interconnect, and unlike the standard PEEC method, we apply the circuit solution technique known as Modified Nodal Analysis in such a manner so that the Block Arnoldi algorithm can be used to produce guaranteed passive reduced order models.

2.1 Integral Equation and Discretization

At each point inside the conductors, we have [7]

$$\boldsymbol{E} = -\nabla\varphi - \frac{\partial \boldsymbol{A}}{\partial t} \tag{2}$$

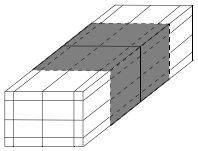

Figure 1: *A discretization of a long and thin conductor only along 1 coordinate direction. Filaments sections are smaller near the surfaces to properly capture skin effect. Panels cover all surfaces (only some are shown).*

where the scalar and vector potentials are, respectively

$$\varphi(\boldsymbol{r}) = \frac{1}{4\pi\epsilon}\int_{V'}\frac{\rho(\boldsymbol{r}')}{\|\boldsymbol{r}-\boldsymbol{r}'\|}dv', \quad (3)$$

$$\boldsymbol{A}(\boldsymbol{r}) = \frac{\mu}{4\pi}\int_{V'}\frac{\boldsymbol{J}(\boldsymbol{r}')}{\|\boldsymbol{r}-\boldsymbol{r}'\|}dv', \quad (4)$$

$\boldsymbol{E}$ is the electric field, ϵ and μ are the electric permittivity and the magnetic permeability of the medium, respectively, V' is the volume of all conductors, ρ is the charge density and $\boldsymbol{J}$ is the current density. Note that we are assuming that the influence of the charge and currents at any point in the structure is instantaneously felt everywhere. This is called the Electromagneto-Quasistatic approximation, which we can assume for structures small compared to the wavelength, as is generally the case for interconnect structures.

To model current flow in the PEEC method, the interior of conductors is divided into a grid of *filaments*, each carrying a constant current density along its length. If the conductor is long and thin, as is often the case with this type of structures, we can assume the length direction as the dominant current flow direction, and use filaments only in that direction, as shown in Figure 1. For plane type structures, one can use a grid of filaments in two coordinate directions. For the general case, without assuming any dominant direction, a 3D grid of filaments must be used. To model charge accumulation, the surface of each conductor is covered with *panels*, each holding a constant charge density. Figure 1 shows only the panels connected to the central node, for simplification.

The combination of the filaments and panels, plus sources, $\boldsymbol{V}_t$, at the terminal pairs, generates a "circuit" whose solution gives the desired admittance parameters, as in the particular case shown in Figure 2. Each of the node points connecting the filaments is a node in the circuit, each filament is a branch of the circuit, as well as each panel, as shown. To generate a system of equations, we first determine the constitutive relations of filaments and panels. To that end, we apply the Galerkin method to the discretized version of (2) (see [6] for details). The constitutive relation for filaments will be

$$\boldsymbol{V}_b^f = (\boldsymbol{R} + j\omega\boldsymbol{L})\boldsymbol{I}_b^f \quad (5)$$

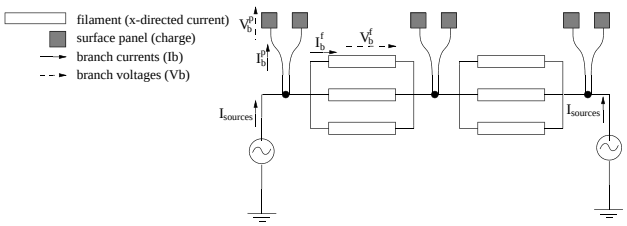

Figure 2: *The "electric circuit" corresponding to the discretization of the conductor in Figure 1. The quantities shown will be used in the MNA formulation.*

where $\boldsymbol{I}_b^f \in \mathbb{C}^f$ is the vector of f filament currents. The $f \times f$ diagonal matrix $\boldsymbol{R}$ of filament DC resistances is defined as

$$R_{ii} = \frac{l_i}{\sigma a_i} \quad (6)$$

where l_i and a_i, are respectively the length and cross section of filament i, and σ is the conductivity of the associated conductor. The matrix of partial inductances, $\boldsymbol{L}$, is the $f \times f$ dense, symmetric positive semidefinite matrix given by

$$L_{ij} = \frac{\mu}{4\pi a_i a_j}\int_{V_i}\int_{V_j'}\frac{\mathbf{l_i}\cdot\mathbf{l_j}}{\|\boldsymbol{r}-\boldsymbol{r}'\|}dv_i'\,dv_j \quad (7)$$

where a_i is the cross section of filament i, V_i is its volume and $\mathbf{l_i}$ is a unit vector with the i^{th} filament length direction (equivalent quantities for filament j). The node potentials come from the panel charges on the surface and are given by

$$\boldsymbol{\Psi}_n = \boldsymbol{P}'\boldsymbol{q}_p \quad (8)$$

where $\boldsymbol{\Psi}_n \in \mathbb{C}^n$ is the vector of the n node voltages, $\boldsymbol{q}_p \in \mathbb{C}^p$ is the charge on each of the p panels, and $\boldsymbol{P}' \in \mathbb{R}^{(n_e+n_i)\times p}$ is the potential coefficients matrix formed by

$$P'_{ij} = \frac{1}{a_j 4\pi\epsilon}\int_{S'_{p_j}}\frac{1}{\|\boldsymbol{r}_i-\boldsymbol{r}'\|}ds'_{p_j} \quad (9)$$

where S'_{p_j} is the surface of panel j, a_j is its area, r_i is the i^{th} node location, n_e is the number of node points on the surface and n_i is the number of internal node points (nodes without any panel connected to it).

Unlike the PEEC method, however, in our formulation we compute the coefficients of potential matrix $\boldsymbol{P}$ in a different way, allowing the verification of charge conservation on every node. $\boldsymbol{P}$ will be computed with:

$$P_{ij} = \frac{1}{a_j 4\pi\epsilon}\int_{S'_{p_j}}\frac{1}{\|\boldsymbol{r}_{p_i}-\boldsymbol{r}'\|}ds'_{p_j}, \quad (10)$$

clearly in the form of partial coefficients of potential, where a_j and p_j are the same as in (9), but $\boldsymbol{r}_{p_i}$ is now the center

of each panel p_i . In our case $\boldsymbol{P} \in \mathbb{R}^{p \times p}$. Note that we allow multiple panels on each node - as is the case for nodes on edges or apices of conductors. Furthermore, we shall see that this form allow us to establish a set of equations amenable to generating passive reduced-order models.

The current flowing onto the panels is given by $\boldsymbol{I}_b^p = j\omega \boldsymbol{q}_p$ (assuming for the sinusoidal steady state), and since the panel node voltages in (8) are voltages relative to infinity, we can view the panel branches as connecting the panel node to the zero potential node at infinity. Then the panel branch voltages are given by $\boldsymbol{V}_b^p = \boldsymbol{\Phi}_p - 0 = \boldsymbol{\Phi}_p$ where $\boldsymbol{\Phi}_p$ are the potentials in the panels. Combining, we get the constitutive relation for panels:

$$\boldsymbol{V}_b^p = \frac{1}{j\omega} \boldsymbol{P} \boldsymbol{I}_b^p \tag{11}$$

With (11) and (5) we can write the constitutive relations for the elements as a single matrix in $\mathbb{C}^{b \times b}$, $b = f + p$,

$$\boldsymbol{V}_b = \begin{bmatrix} \boldsymbol{V}_b^f \\ \boldsymbol{V}_b^p \end{bmatrix} = \begin{bmatrix} \boldsymbol{R} + j\omega \boldsymbol{L} & 0 \\ 0 & \boldsymbol{P}/(j\omega) \end{bmatrix} \begin{bmatrix} \boldsymbol{I}_b^f \\ \boldsymbol{I}_b^p \end{bmatrix} = \boldsymbol{Z} \boldsymbol{I}_b. \tag{12}$$

2.2 Applying Modified Nodal Analysis

We can now apply Kirchoff's Voltage and Current Laws via the circuit solution technique known as Modified Nodal Analysis to derive a system of equations whose solution gives $\boldsymbol{Y}_t$. Note that we will only use voltage sources because one needs to connect all the sources to the zero potential node at infinity and that node is only connected to capacitors. This is necessary in order to be able to use Model Order Reduction techniques with expansions around $s = 0$ (a DC solution is desirable if we want to use the model in time-domain simulations).

Kirchoff's Current Law, which implies that the sum of the branch currents leaving each node in the network must be zero, is represented by

$$\begin{bmatrix} \boldsymbol{A} & -\boldsymbol{N} \end{bmatrix} \begin{bmatrix} \boldsymbol{I}_b \\ \boldsymbol{I}_{src} \end{bmatrix} = \begin{bmatrix} 0 \end{bmatrix} \tag{13}$$

where $\boldsymbol{A} \in \mathbb{R}^{n \times t}$ is the sparse nodal incidence matrix summing the filament and panel currents leaving each node, $\boldsymbol{N} \in \mathbb{R}^{n \times n_{src}}$ is the sparse matrix summing the currents through the voltage sources, n is the number of nodes (excluding the one for the point at infinity), t is the number of filaments plus panels (each of these elements forms a branch in the circuit), and n_{src} is the number of voltage sources in the circuit (same as k in the beginning of this section). $\boldsymbol{I}_b \in \mathbb{R}^t$ is the vector of branch currents, $\boldsymbol{I}_{src} \in \mathbb{R}^{n_{src}}$ is the vector of currents leaving each voltage source (always connected to ground) and entering the nodes. Note the 0 in the right hand side due to the inexistence of any current source in the circuit.

Applying Kirchoff's Voltage Law to the circuit, we obtain

$$\begin{bmatrix} \boldsymbol{A}^T \\ \boldsymbol{N}^T \end{bmatrix} \begin{bmatrix} \boldsymbol{V}_n \end{bmatrix} = \begin{bmatrix} \boldsymbol{V}_b \\ \boldsymbol{V}_{src} \end{bmatrix} \tag{14}$$

where $\boldsymbol{V}_n$ is the vector of voltages at each node in the network, $\boldsymbol{V}_{src}$ are the known source voltages, and $\boldsymbol{V}_b$ is the vector of voltages at each branch (filaments or panels). See Figure 2 for an illustration of these quantities.

Note that $\boldsymbol{V}_{src}$ is exactly the terminal voltage vector $\boldsymbol{V}_t$, from (1). $\boldsymbol{I}_t$ will be equal to $\boldsymbol{I}_{src}$.

Combining (14) with (13) and (12) yields the system of equations

$$\begin{bmatrix} \boldsymbol{Z} & -\boldsymbol{A}^T & 0 \\ \boldsymbol{A} & 0 & -\boldsymbol{N} \\ 0 & \boldsymbol{N}^T & 0 \end{bmatrix} \begin{bmatrix} \boldsymbol{I}_b \\ \boldsymbol{V}_n \\ \boldsymbol{I}_{src} \end{bmatrix} = \begin{bmatrix} 0 \\ 0 \\ \boldsymbol{V}_{src} \end{bmatrix} \tag{15}$$

To accurately capture frequency dependent effects for time domain circuit simulation, (15) could be solved for specific frequencies, and then a rational fitting algorithm can be used to compute a model for the package [8, 9]. Another approach is to include a sparse tableau version of (15) in a circuit simulator instead of solving for the terminal behavior [6]. However, even with the approximations in this section (assuming dominant directions for the current flow) the size of (15) becomes extremely large if high accuracy is desired, and these methods become computationally intractable. Instead, it is necessary to reduce the size of system through a model order reduction technique which is the topic of the next section.

3 Coupled Circuit-Interconnect Simulation and Passive Model Order Reduction

The basic idea of MOR techniques is to reduce the size of the system described by the circuit equations, usually written in a convenient state-space form, to a much smaller one that still captures the dominant behavior of the original system. This approximation is then used to generate a model to be inserted in a circuit simulator such as SPICE or SPECTRE. The field of MOR has matured significantly in the past few years. Recently, MOR techniques, such as the PRIMA algorithm [10], have been presented, that are guaranteed to produce stable and passive reduced-order models. To apply this algorithm, the circuit equations are written in state-space form

$$\begin{aligned} s\boldsymbol{\mathcal{L}}\,\boldsymbol{x} &= -\boldsymbol{\mathcal{R}}\,\boldsymbol{x} + \boldsymbol{B}\,\boldsymbol{u} \\ \boldsymbol{y} &= \boldsymbol{B}^T \boldsymbol{x}. \end{aligned} \tag{16}$$

where $s = j\omega$.

To derive a state space form of (15), the powers of the Laplace variable $s = j\omega$ must all be to the first power only. However, the $\boldsymbol{Z}$ matrix in (12) contains terms with both s and $1/s$. To separate the $1/s$ power, note first that as seen in Figure 2, the branch currents can be categorized into two types, $\boldsymbol{I}_b = [\boldsymbol{I}_b^f; \boldsymbol{I}_b^p]$ where $\boldsymbol{I}_b^f$ represents the currents in filaments and $\boldsymbol{I}_b^p$ represents the currents onto panels. Also, consider separating $\boldsymbol{A}$ into $[\boldsymbol{A}_e; \boldsymbol{A}_i]$ where the lines of $\boldsymbol{A}_e$ corresponds to the n_e external nodes and $\boldsymbol{A}_i$ corresponds to the n_i internal nodes. Based on this categorization, (13) becomes

$$\begin{bmatrix} \boldsymbol{A}_e & \boldsymbol{B}_e & -\boldsymbol{N}_e \\ \boldsymbol{A}_i & 0 & 0 \end{bmatrix} \begin{bmatrix} \boldsymbol{I}_b^f \\ \boldsymbol{I}_b^p \\ \boldsymbol{I}_{src} \end{bmatrix} = \begin{bmatrix} 0 \\ 0 \end{bmatrix} \qquad (17)$$

The zero-blocks correspond to $\boldsymbol{B}_i$ and $\boldsymbol{N}_i$, which are always null since there are no panels or voltage sources connected to internal nodes. We can also rewrite (14) separating the branch voltages in $\boldsymbol{V}_b = [\boldsymbol{V}_b^f; \boldsymbol{V}_b^p]$. $\boldsymbol{V}_n^e$ and $\boldsymbol{V}_n^i$ correspond to the voltages in external and internal nodes, respectively.

$$\begin{bmatrix} \boldsymbol{A}_e^T & \boldsymbol{A}_i^T \\ \boldsymbol{B}_e^T & 0 \\ \boldsymbol{N}_e^T & 0 \end{bmatrix} \begin{bmatrix} \boldsymbol{V}_n^e \\ \boldsymbol{V}_n^i \end{bmatrix} = \begin{bmatrix} \boldsymbol{V}_b^f \\ \boldsymbol{V}_b^p \\ \boldsymbol{V}_{src} \end{bmatrix} \qquad (18)$$

The desired equation in state-space form must now be built using these last two matrix equations plus the constitutive relations expressed in (12). Using the first equation in (17) and the constitutive relation for panels, we can write

$$\boldsymbol{A}_e \boldsymbol{I}_b^f + s\boldsymbol{B}_e \boldsymbol{P}^{-1} \boldsymbol{V}_b^p - \boldsymbol{N}_e \boldsymbol{I}_{src} = 0 \qquad (19)$$

Furthermore, using the second relation in (18), we have

$$\boldsymbol{A}_e \boldsymbol{I}_b^f + s\boldsymbol{B}_e \boldsymbol{P}^{-1} \boldsymbol{B}_e^T \boldsymbol{V}_n^e - \boldsymbol{N}_e \boldsymbol{I}_{src} = 0 \qquad (20)$$

On the other hand, using the constitutive relation for filaments with the first relation in (18), yields

$$(\boldsymbol{R} + s\boldsymbol{L})\boldsymbol{I}_b^f - \boldsymbol{A}_e^T \boldsymbol{V}_n^e - \boldsymbol{A}_i^T \boldsymbol{V}_n^i = 0 \qquad (21)$$

Using (20) and (21) plus the relations not yet used in (17) and (18), and separating the terms multiplying s, we obtain the state-space form:

$$s \begin{bmatrix} \boldsymbol{L} & 0 & 0 & 0 \\ 0 & \boldsymbol{B}_e \boldsymbol{P}^{-1} \boldsymbol{B}_e^T & 0 & 0 \\ 0 & 0 & 0 & 0 \\ 0 & 0 & 0 & 0 \end{bmatrix} \begin{bmatrix} \boldsymbol{I}_b^f \\ \boldsymbol{V}_n^e \\ \boldsymbol{V}_n^i \\ \boldsymbol{I}_{src} \end{bmatrix} =$$

$$- \begin{bmatrix} \boldsymbol{R} & -\boldsymbol{A}_e^T & -\boldsymbol{A}_i^T & 0 \\ \boldsymbol{A}_e & 0 & 0 & -\boldsymbol{N}_e \\ \boldsymbol{A}_i & 0 & 0 & 0 \\ 0 & \boldsymbol{N}_e^T & 0 & 0 \end{bmatrix} \begin{bmatrix} \boldsymbol{I}_b^f \\ \boldsymbol{V}_n^e \\ \boldsymbol{V}_n^i \\ \boldsymbol{I}_{src} \end{bmatrix} + \begin{bmatrix} 0 \\ 0 \\ 0 \\ \boldsymbol{V}_{src} \end{bmatrix}$$

which is clearly in a form similar to Eqn. (16).

Note that we can avoid computing $\boldsymbol{P}^{-1}$ explicitly, which is computationally expensive, using a recycled Krylov-subspace iterative algorithm, as described in [11, 12]. To generate passive reduced order models as in [10, 13, 14], it is enough that $\boldsymbol{\mathcal{R}}$ is positive semidefinite while $\boldsymbol{\mathcal{L}}$ must be positive semidefinite.

$\boldsymbol{L}$ is positive definite. If $\boldsymbol{P}$ is generated via a Galerkin approach, then it too is positive definite, and so is $\boldsymbol{B}_e \boldsymbol{P}^{-1} \boldsymbol{B}_e^T$. Since $\boldsymbol{\mathcal{L}}$ is a block diagonal matrix consisting of blocks which are each positive semidefinite, then so is $\boldsymbol{\mathcal{L}}$.

For $\boldsymbol{\mathcal{R}}$ to be positive semidefinite, $\boldsymbol{x}^T \boldsymbol{\mathcal{R}} \boldsymbol{x} \geq 0$ for any $\boldsymbol{x}$. Let $\boldsymbol{x} = [\boldsymbol{u}^T \boldsymbol{v}^T \boldsymbol{y}^T \boldsymbol{z}^T]^T$, then

$$\begin{aligned} \boldsymbol{x}^T \boldsymbol{\mathcal{R}} \boldsymbol{x} &= (\boldsymbol{u}^T \boldsymbol{R} + \boldsymbol{v}^T \boldsymbol{A}_e + \boldsymbol{y}^T \boldsymbol{A}_i)\boldsymbol{u} - \\ &\quad (\boldsymbol{u}^T \boldsymbol{A}_e^T - \boldsymbol{z}^T \boldsymbol{N}_e^T)\boldsymbol{v} - \boldsymbol{u}^T \boldsymbol{A}_i^T \boldsymbol{y} - \boldsymbol{v}^T \boldsymbol{N}_e \boldsymbol{z} \\ &= \boldsymbol{u}^T \boldsymbol{R} \boldsymbol{u} \geq 0 \end{aligned}$$

since $\boldsymbol{R}$ is positive semidefinite.

The number of states in this nodal formulation in the presented state-space form is $f + n + n_{src}$, where f is the number of filaments, n is the number of nodes (internal + external) and n_{src} is the number of sources.

4 Formulation Results

To verify that our nodal formulated parasitic extraction program gives correct results, we first present a comparison between a time-domain simulation using our model and experimental measurements. Figure 3 shows a real connector structure from Teradyne Inc. composed of 18 pins with a ground shield around and between the conductors. For this experiment all pins are connected to ground through resistors. Then a noisy input is connected in series with one of these resistors and a step with a $500ps$ rise-time is imposed on it. The voltage waveform at an adjacent pin is collected. Figure 4 shows the waveform measured at that pin and compares it with results of a time-domain simulation performed using a 140^{th} order reduced model computed from a 742^{th} order model. As can be seen from the plot the waveforms are qualitatively similar and acceptable accuracy is obtained. If higher accuracy is required, a finer discretization can be used.

Let us now analyze the efficiency of the Model Order Reduction algorithm. Figure 5 shows the impedance frequency response of one pin of the same connector, using a simple discretization of 150 filaments and 2400 panels, for different order reduced models. These responses were computed with our nodal formulation in the Model Order Reduction algorithm using moment matching at $s = 0$. The

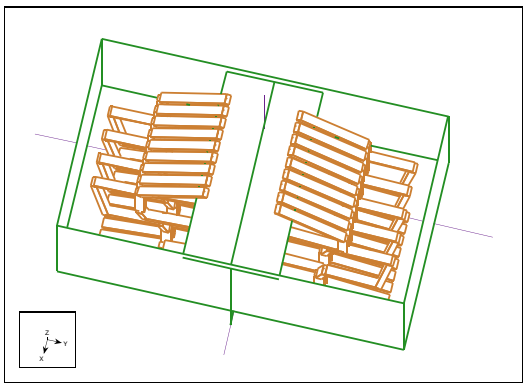

Figure 3: *A 3D connector*

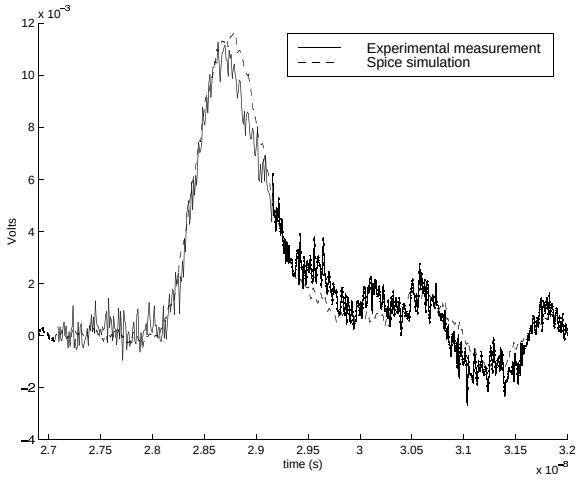

Figure 4: *Comparison between measured time-domain waveforms and simulated results obtained using a reduced-order model of the connector example.*

full system has 352 states. In the figure, models with orders 94 and 246 are compared to the exact response. Note the strong improvement from 94 to 246 states. Although we can see that for increasing size models we match the full model response in a larger range of frequencies, and that we can actually compute accurate reduced-order models, their sizes need to be larger than what we could expect.

To understand what is happening, let us consider a very simple structure composed of two long and thin conductors, as show in Figure 6. Both conductors are $1cm$ long, $37\mu m$ wide, $13\mu m$ in height and the distance between them is $17\mu m$. The structure is discretized in 416 panels and 150 filaments producing a 323^{th} order model. Figure 7 shows the magnitude of the frequency dependent impedance of both the full system and of a 62^{th} order reduced model using $s = 0$ as the expansion point. Figure 8 shows the positioning of the system and reduced model poles. Notice the relatively large number of real poles near the origin

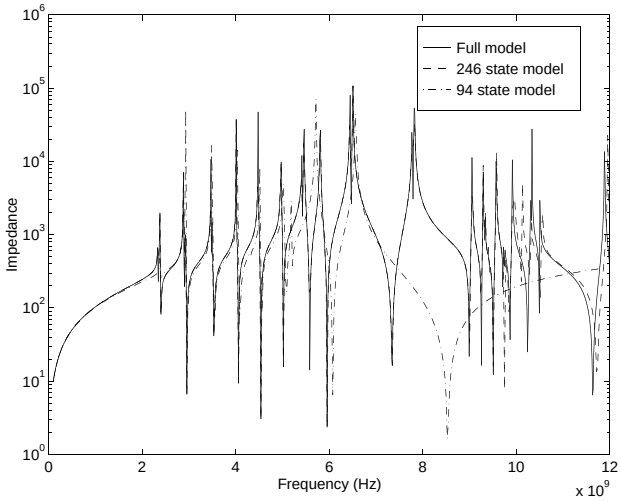

Figure 5: *Various reduced order models for the connector*

Figure 6: *A simple example geometry.*

(observe the scaling of the plot). The real poles correspond to the added modes resulting from the discretization of the conductor into bundles of filaments. The effect of this large cluster of poles (in this case about 90% of all poles) near the origin is weak. In fact, all of these poles are nearly or exactly canceled by zeros and thus do not have a strong effect on the response. These weak poles are then responsible for the large orders required for any general PEEC-based model. The choice of one or several expansion points away from $s = 0$ could be a solution but that is computationally more expensive and it is not obvious what points to choose. Furthermore, a correct solution near $s = 0$ (DC solution) is essential to time-domain simulation. Efficient and generic ways to overcome this difficulty are currently under investigation.

5 Conclusions

In this paper we showed that the PEEC method combined with Modified Nodal Analysis can be used in a guaranteed passive model order reduction algorithm to model three-dimensional interconnect structures. A reduced-order model based on this formulation was shown to produce the correct results for a real connector example. The difficulties in obtaining low-order reduced models for these PEEC-based models were described and directions for further research were presented.

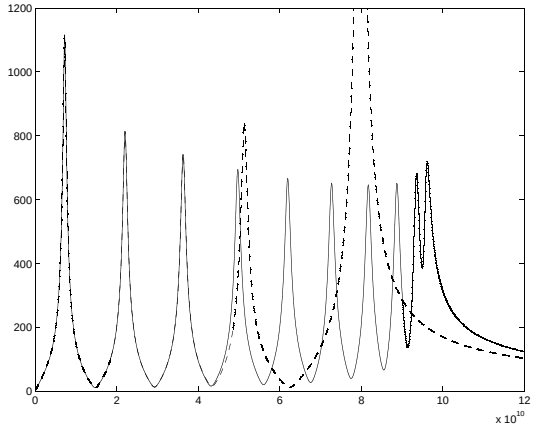

Figure 7: *Magnitude of the impedance response for the simple geometry using the nodal formulation with an expansion point in $s = 0$.Continuous line: full system; dashed line: reduced model.*

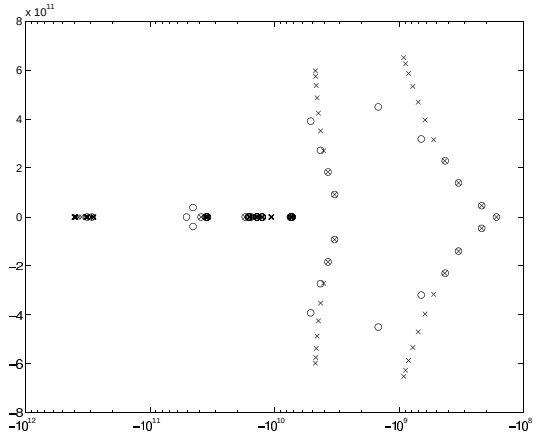

Figure 8: *Positioning of the system ($\times$) and reduced model ($\circ$) poles for the simple geometry.*

Acknowledgments

The authors would like to thank Mike Tsuk of Digital Equipment Corp. for the practical example. This work was partially supported by the Defense Advanced Research Projects Agency, the National Science Foundation, the Portuguese JNICT programs PRAXIS XXI and FEDER under contracts 2/2.1/T.I.T/1661/95 and 2/2.1/T.I.T/1639/95 and grant BM-8592/96.

References

[1] K. Nabors and J. White. Fast capacitance extraction of general three-dimensional structures. *IEEE Trans. on Microwave Theory and Techniques*, June 1992.

[2] M. Kamon, M. J. Tsuk, and J. White. Fasthenry, a multipole-accelerated 3-d inductance extraction program. In *Proceedings of the ACM/IEEE Design Automation Conference*, Dallas, June 1993.

[3] L. Greengard and V. Rokhlin. A fast algorithm for particle simulations. *Journal of Computational Physics*, 73(2):325–348, December 1987.

[4] J. R. Phillips. Error and complexity analysis for a collocation-grid-projection plus precorrected-FFT algorithm for solving potential integral equations with Laplace or Helmholtz kernels. In *Proceedings of the 1995 Copper Mountain Conference on Multigrid Methods*, April 1995.

[5] C. Desoer and E. Kuh. *Basic Circuit Theory*. McGraw-Hill, New York, 1969.

[6] Albert E. Ruehli. Equivalent Circuit Models for Three-Dimensional Multiconductor Systems. *IEEE Transactions on Microwave Theory and Techniques*, MTT-22(3):216–221, March 1974.

[7] E. C. Jordan and K. G. Balmain. *Electro-Magnetic Waves and Radiating Systems*. Prentice-Hall, Englewood Cliffs, N.J., 1968.

[8] L. Miguel Silveira, Ibrahim M. Elfadel, Jacob K. White, Monirama Chilukura, and Kenneth S. Kundert. Efficient Frequency-Domain Modeling and Circuit Simulation of Transmission Lines. *IEEE Transactions on Components, Packaging, and Manufacturing Technology – Part B: Advanced Packaging*, 17(4):505–513, November 1994.

[9] Tuyen V. Nguyen, Jing Li, and Zhaojun Bai. Dispersive coupled transmission line simulation using an adaptive block lanczos algorithm. In *International Custom Integrated Circuits Conference*, pages 457–460, 1996.

[10] Altan Odabasioglu, Mustafa Celik, and Lawrence Pileggi. Prima: Passive reduced-order interconnect macromodeling algorithm. In *International Conference on Computer Aided-Design*, pages 58–65, San Jose, California, November 1997.

[11] R. Telichevesky, K. Kundert, and J White. Efficient AC and noise analysis of two-tone RF circuits. In *Proceedings 33rd Design Automation Conference*, Las Vegas, Nevada, June 1996.

[12] J. R. Phillips, E. Chiprout, and D. D. Ling. Efficient full-wave electromagnetic analysis via model-order reduction of fast integral transforms. In *Proceedings 33rd Design Automation Conference*, Las Vegas, Nevada, June 1996.

[13] E. Bracken. Passive modeling of linear interconnect networks. *IEEE Transactions on Circuits and Systems, Part I: Fundamental Theory and Applications, to appear*.

[14] K. J. Kerns, I. L. Wemple, and A. T. Yang. Stable and efficient reduction of substrate model networks using congruence transforms. In *IEEE/ACM International Conference on Computer Aided Design*, pages 207 – 214, San Jose, CA, November 1995.